J. Membrane Biol. 56, 9–18 (1980)

The Journal of
Membrane Biology

Frequency Entrainment of Squid Axon Membrane

Rita Guttman, Lance Feldman, and Eric Jakobsson

Brooklyn College of the City University of New York, Brooklyn, New York 11210, Marine Biological Laboratory, Woods Hole, Massachusetts 02543, and Department of Physiology and Biophysics, University of Illinois, Urbana, Illinois 61801

Summary. Sinusoidally varying stimulating currents were applied to space-clamped squid giant axon membranes in a double sucrose gap apparatus. Stimulus parameters varied were peak-to-peak current amplitude, frequency, and DC offset bias. In response to these stimuli, the membranes produced action potentials in varying patterns, according to variation of input stimulus parameters. For some stimulus parameters the output patterns were stable and obviously periodic with the periods being simple multiples of the input period; for other stimulus parameters no obvious periodicity was manifest in the output. The experimental results were compared with simulations using a computer model which was modified in several ways from the Hodgkin-Huxley model to make it more representative of our preparation. The model takes into account K^+ accumulation in the periaxonal space, features of Na^+ inactivation which are anomalous to the Hodgkin-Huxley model, sucrose gap hyperpolarization current, and membrane current noise. Many aspects of the experiments are successfully simulated but some are not, possibly because some very slow process present in the preparation is not included in the model.

One way to characterize the signal-handling characteristics of a device for transmitting information (such a device as, e.g., a neuron) is by determining the frequency response. Computations of the Hodgkin-Huxley model for the squid axon as subjected to a sinusoidally varying current stimulation were related by Nemoto et al. (1975) to experimental observations on mechanoreceptors. Additional computations on the Hodgkin-Huxley axon for other values of sinusoidally varying stimulating parameters were done by Holden (1976). The sinusoidally driven H-H model behaves in some ways similar to a forced Van der Pol oscillator (Flaherty & Hoppenstadt, 1978).

Partly because of the above theoretical work, and partly because of the inherent aptness of frequency response as a mode of analyzing signalling devices, we have done experiments in which the squid axon (the biological analogue to the H-H model) is sinusoidally driven. As an aid in understanding our results, we have done some computer simulations of our preparation. However, we have not used the unmodified H-H model to do our simulations, because there are several specific ways in which we know that model is an imperfect representation of our system. These ways are as follows:

i) K^+ accumulation in the periaxonal space of squid axons alters the response to sustained stimulating currents, mainly because of the effect of extracellular K^+ concentration on Na^+ inactivation (Adelman & Palti, 1969; Adelman & FitzHugh, 1975). We have incorporated into our simulations the Na^+ inactivation modifications suggested by Adelman and FitzHugh.

ii) An extra diffusion potential due to the presence of the flowing sucrose solutions leads to a substantial hyperpolarization of the membrane in the test pool (Julian, Moore & Goldman, 1962). In our simulations we have set the reversal potential for the leakage current at a more hyperpolarized level and increased the magnitude of the leakage conductance.

iii) The inactivation of the sodium conductance is not accurately described by the Hodgkin-Huxley model. A brief review of the experimental literature on the Na^+ inactivation anomalies is given in Jakobsson, 1978*a*. Possible effects of the inactivation anomalies on response to sustained stimulation are given in Jakobsson, 1978*b*. Because these effects seem likely to be significant in describing response to sinusoidal stimulation, we have done most of our simulations with the Jakobsson (1978*a*, *b*) model for the Na^+ channels rather than the Hodgkin-Huxley one. We have modified the Jakobsson model for K^+ accumulation in just the same way that Adelman and Fitz-

0022-2631/80/0056-0009 $02.00

Hugh (1975) modified the H-H model. (Details of simulations including equations with numerical parameters are displayed in the Appendix).

iv) Noise is not usually taken into account in simulations of excitable membrane behavior, but it is known that noise may modify apparent thresholds for excitation. In analyzing sinusoidal stimulation threshold is particulary important, since we found that the spiking frequency may change abruptly for a very small change in stimulus frequency or intensity at many locations in the stimulus parameter space. Thus as we vary the stimulus parameters we effectively cross many thresholds in a single experiment. To get at least a rough idea of the effect of membrane noise on these threshold behaviors, we imposed a sum of sinusoidal currents to approximate the power spectrum of membrane current noise associated with conductance fluctuations in squid axon as reported by Fishman, Moore and Poussart, 1975. (Details of simulations including equations with numerical parameters are displayed in the Appendix.)

Experimental Methods

The giant nerve fiber of the hindmost stellar nerve of the squid *Loligo pealei* was used throughout. It was dissected under running seawater, separated from neighboring small fibers under a binocular dissection microscope, dipped in an isosmotic deionized sucrose solution (800 mM) for a few seconds, blotted on tissue, and then mounted in a Lucite chamber which was described in a previous paper (Guttman, 1969). The chamber consisted of five compartments: *A*, *B*, *C*, *D*, and *E*. The ends of the axons were secured in compartments *A* and *E* and spanned compartments *B*, *C*, and *D*. Compartments *A* and *E* contained 400 mM KCl, in effect depolarizing the ends of the axon; *B* and *D* contained flowing isosmotic sucrose (800 mM) and isolated compartment *C*, which contained flowing Tris-buffered artificial seawater (430 mM NaCl, 10 mM KCl, 10 mM $CaCl_2$, 50 mM $MgCl_2$, 5 mM Tris). The axon was stimulated by means of platinized platinum electrodes placed in compartments *A* and *C*. The membrane potential was measured by means of chloridized silver electrodes placed in compartments *C* and *E*. A current clamp of the patch of axon membrane, isolated by the flowing sucrose streams, was achieved by means of a 1.3 MΩ "swamping" resistor. The membrane was effectively space-clamped by virtue of the narrow experimental portion in compartment *C* (about 1 mm).

The stimulus consisted of gated sinusoidal current superimposed on current steps of various magnitudes. The stimulus waveform was generated by means of a Wavetek Model 185 Function Generator (Wavetek, San Diego, Calif.) used in the gated normal operation mode. The gating waveform to the Wavetek Model 185 was provided by a Hewlett Packard 9010 A Pulse Generator. The gating waveform had a duty factor of 0.1 with $t = 500$ msec of stimulus separated by 4.5 sec of rest. The period of the stimulating sinusoid was measured on line by means of a Tektronix DC 504 Digital Computer/Timer. The stimulus and response were displayed on a Tektronix 564 B Storage Oscilloscope operated in the externally triggered, autoerase storage mode.

A trigger waveform generated internally by the Tektronix 564 B Storage Oscilloscope synchronized the gating waveform and the time base and autoerase circuits of the Tektronix 546 B storage oscilloscope. Thus a "fresh" record was provided with each stimulus.

The stimulus current and membrane voltage response were also recorded in analog form on magnetic tape by use of a Hewlett-Packard 3960 A Tape Recorder. The membrane voltage response was measured by means of the Ag/AgCl electrodes in compartments *C* and *E* which input to custom-built impedance convertors and difference amplifier. Membrane resting potential was measured by use of Data Precision Model 245 TriPhasic Digital Multimeter (Data Precision, Wakefield, Mass.). Temperature was measured by use of the Bailey Instruments Model BAT-8 Amplifier Compensated Thermocouple Digital Thermometer (Bailey Instruments Co., Inc., Saddlebrook, N.J.).

Off-line analysis was accomplished from paper chart records obtained by reproducing the data stored on magnetic tape at reduced speed and transferring them onto a Brush Model 220 Paper Chart Recorder (Gould Inc., Instrument Systems Division, Cleveland, Ohio).

In a portion of the work, transient patterns at the onset of stimulation were studied. In another part of the work, the "steady-state" system properties were determined by ignoring the first 100 msec of the record after stimulus onset and then counting the spikes in the remainder of the record. Then the ratio of the number of spikes to the total number of driving cycles was calculated. In most cases a regular pattern of spikes and "misses" (a "miss" is defined as a time interval which contains a full driving cycle but no spike) was encountered, but in some no pattern was discernible to the eye.

In all, experiments were performed on 18 axons, with many runs carried out on each axon. Temperature was varied between 9 and 18 °C, but during any one run there was usually not more than about 0.1 °C variation in temperature.

Experimental Results

A convenient way to represent the results of sinusoidal current stimulation is by a *rotation number*,

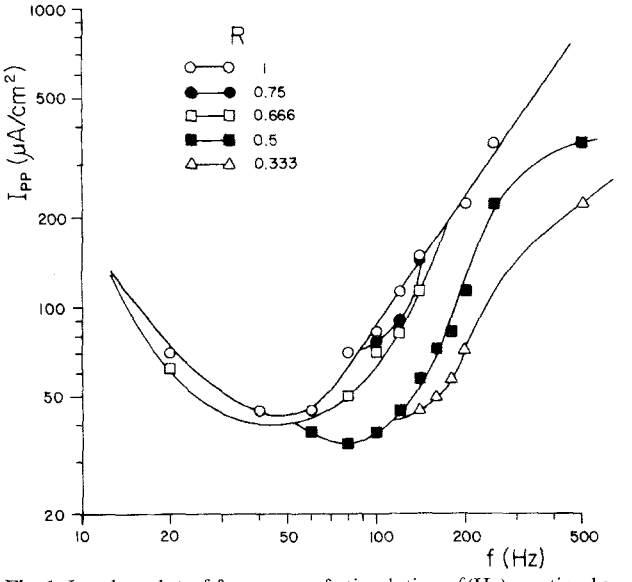

Fig. 1. Log-log plot of frequency of stimulation, f(Hz) *vs.* stimulus current intensity (μA/cm²) for various steady-state rotation ratios, *R*. DC offset = 10.8 μA/cm². Each curve represents the lowest intensity at which the respective rotation ratio occurs. All data points were taken on same axon at 10 °C. Same data as Table 1.

Table 1. R as a function of frequency and intensity of stimulation for squid axons

Stimulus intensity ($\mu A/cm^2$)[a]	Frequency (Hz)														
	20	40	60	80	100	120	140	160	180	200	250	300	350	400	500
34.2	0	0	0.134	0.5	0.118	0									
37.8	0	0	0.5	0.5	0.5	0.182	0								
41.4	0	0.871	0.772	0.5	0.5	0.414	0.2	0	0	0					
45.0	0	1	1	0.527	0.5	0.5	0.333	0.122	0	0					
50.4	0		1	0.667	0.5	0.5	0.377	0.333	0.108	0					
54.0	0	1	1	0.881	0.5	0.5	0.473	0.333	0.174	0					
57.6	0	1	1	0.787	0.5	0.5	0.5	0.324	0.333	0.118					
62.1	0.64	1	1	0.920	0.5	0.5	0.5	0.336	0.342	0.161					
70.2	1	1	1	1	0.667	0.5	0.5	0.469	0.333	0.321					
72.9	1	1	1	1	0.667	0.5	0.5	0.5		0.333					
77.4	1	1	1	1	0.75	0.5	0.5	0.5		0.333					
82.8	1	1	1	1	1	0.667	0.5	0.5	0.5	0.333					
86.4	1	1	1	1	1	0.667	0.5	0.5	0.5						
90.0	1	1	1	1	1	0.75	0.5	0.5	0.5						
113.4	1	1	1	1	1	1	0.667	0.5	0.5	0.5					
148.5	1	1	1	1	1	1	1	0.75	0.5	0.5					
220.5	1	1	1	1	1	1	1	1	1	1	0.5	0.5	0.5	0.5	0.333
351.0	1	1	1	1	1	1	1	1	1	1	1	0.5	0.5	0.5	0.5

[a] On a DC bias of 10.8 $\mu A/cm^2$.
The lowest intensity at which a particular apparently rational R was first detected is underlined.

R, defined as the ratio of the number of spikes produced by the membrane to the number of cycles in the forcing current. A pattern of steady-state R's observed for a typical axon with various stimulation current parameters is shown graphically in Fig. 1, and in tabular form in Table 1. It is noteworthy that $R>1$ was never observed. Also noteworthy is that while most R's were simple rational numbers (i.e., 1/3, 1/2, 2/3, 3/4), some R's were not. In the cases where $R=m/n$, with "m" and "n" small integers, the responses were periodic with a period nP_i where P_i is the input period. In the cases where R was not simply rational, the output was not obviously periodic.

Current and voltage records for one of the Table 1 current values, (72.9 $\mu A/cm^2$), are shown in Fig. 2 for 40, 100, 120, and 200 Hz. Several typical features of the response patterns can be seen. Note that when $R=2/3$, the second of each pair of successive spikes is smaller than the first. Also the second spike lags its driving current cycle by more than the first. When $R=1/3$, the second of each pair of successive subthreshold oscillations is larger than the first. These features were general in obviously periodic responses which involved spike generation in consecutive driving cycles; the spike amplitudes successively decreased with each driving cycle until the spike "failed". In those obviously periodic responses which involved subthreshold responses in consecutive driving cycles, the response amplitudes successively increased until the last one finally "broke out" into a spike. The effects of varying DC bias current are shown in Figs. 3 and 4. In Fig. 3 rotation ratio *vs.* amplitude of sinusoidal current variation is plotted for various values of DC bias current, to give a picture of how the system responds to variations in the three quantities which characterize the stimulus: peak current amplitude, frequency, and DC bias. (Figures 3 and 4 represent data from a different axon than Figs. 1 and 2.)

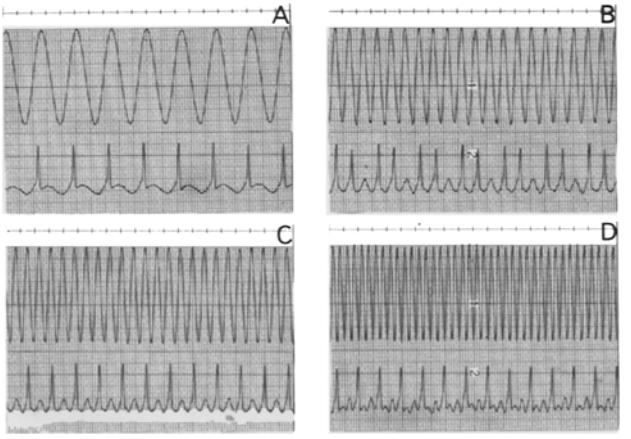

Fig. 2. Steady-state membrane response to a 72.9 $\mu A/cm^2$ peak-to-peak sinusoidal stimulus upon a DC bias of 10.8 $\mu A/cm^2$, illustrating phase locking. (*A*): $f=40$ Hz; $R=1$. (*B*): $f=100$ Hz; $R=0.667$. (*C*): $f=120$ Hz; $R=0.5$. (*D*): $f=200$ Hz; $R=0.333$. Upper trace is current stimulus. Lower trace is membrane voltage response. All data on same axon at 10 °C.

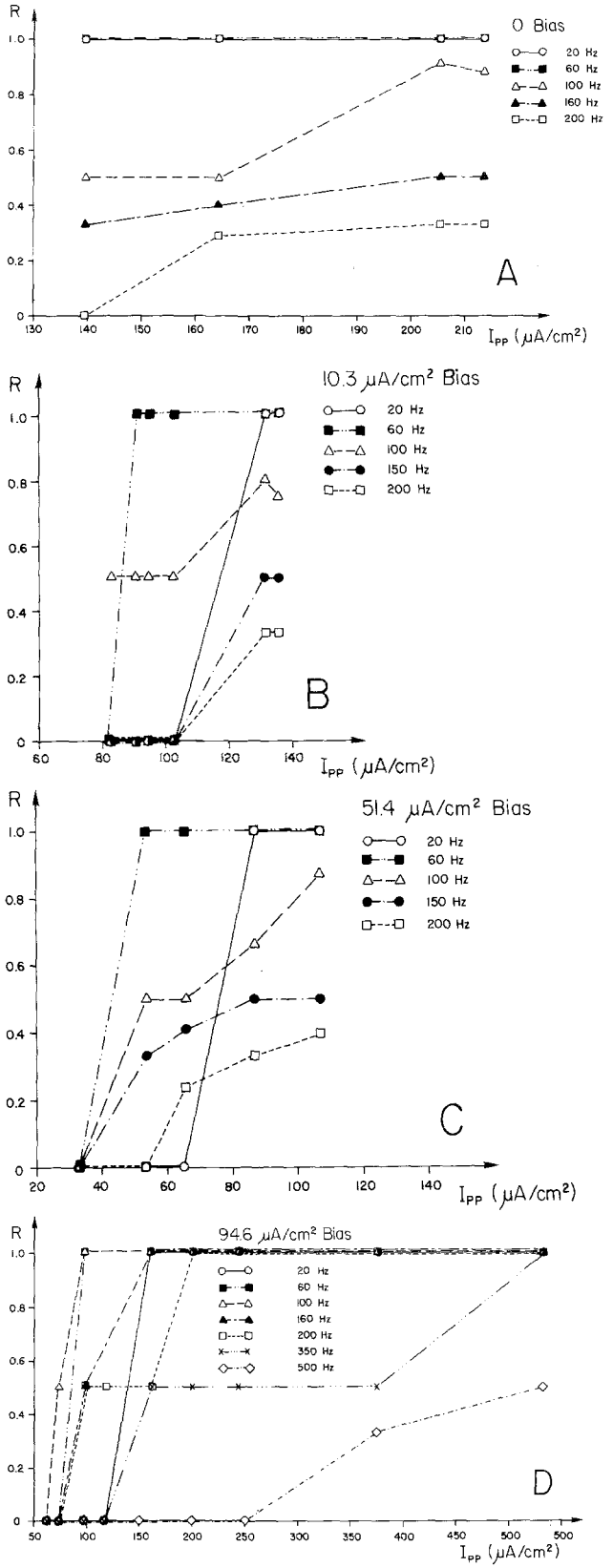

Fig. 3. Intensity-response curves for space-clamped squid axon stimulated by a sinusoidal current of various frequencies on DC bias of; (*A*): zero, (*B*) 10.3 μA/cm², (*C*) 51.4 μA/cm², and (*D*) 94.6 μA/cm². All curves were taken on the same axon. Temperature is 12 °C.

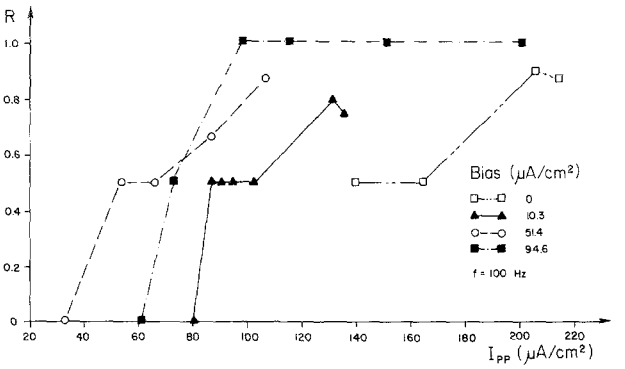

Fig. 4. Effect of magnitude of DC bias upon intensity-response curve for space-clamped squid axon stimulated by a sinusoidal current at a frequency of 100 Hz. Temperature is 12 °C. Same data as Fig. 3.

Figure 4 is some of the data of Fig. 3 plotted in a slightly different way to show the dual effect of the DC bias current. Up to a certain value the depolarizing DC bias current enhances spiking in the response (increases R) but at 94.6 μA/cm² this trend has partly reversed. We believe that this is largely because the steady depolarizing current causes inactivation of the sodium channels. The dual effect of DC bias current on R is a reflection in frequency response of "the dual effect of membrane potential on sodium conductance in the giant axon of *Loligo*" (Hodgkin & Huxley, 1952).

For the membrane functioning at any particular value of R, if the current is held constant and the frequency increased, the spike lags farther and farther behind the peak driving current in the cycle, until finally the spike is "missed" and the membrane enters into a new "R domain". An example of the phase relationship between spike and driving current as a function of frequency is given in Fig. 5. The Hodgkin-Huxley model behaves in precisely the same way as the real membrane in this regard (Holden, 1976).

Figure 6 shows the behavior at boundaries between R-domains for one axon stimulated with a peak-to-peak current of 181 μA/cm² (0 DC bias) and various frequencies. Several features of this figure are noteworthy. For one thing, at this frequency for this axon there are no R-values between $R=1$ and $R=1/2$, nor between $R=0.5$ and $R=0.25$. Further, the transition between R-domains occurs by a gradedness of the size of response rather than by a change in the number of full-sized responses; i.e., instead of some spikes disappearing at a particular frequency, it rather occurs that every second spike gets smaller, with the size being a continuous function of the frequency. A different sort of behavior near transition boundaries between R-domains is seen in Fig. 7*a* and *b*. There we see the system evolving to its steady-state

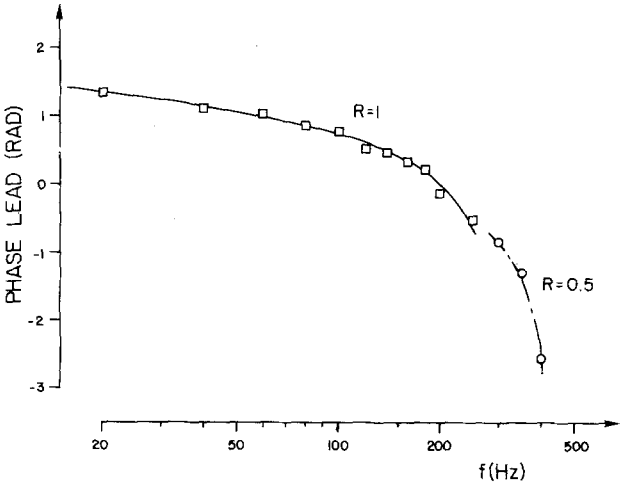

Fig. 5. Phase angles of phase-locked action potentials when $R=1$ and $R=0.5$, respectively, when axon is stimulated by a sinusoidal current of 220.5 $\mu A/cm^2$ on a DC bias of 10.8 $\mu A/cm^2$ at a temperature of 10.3 °C.

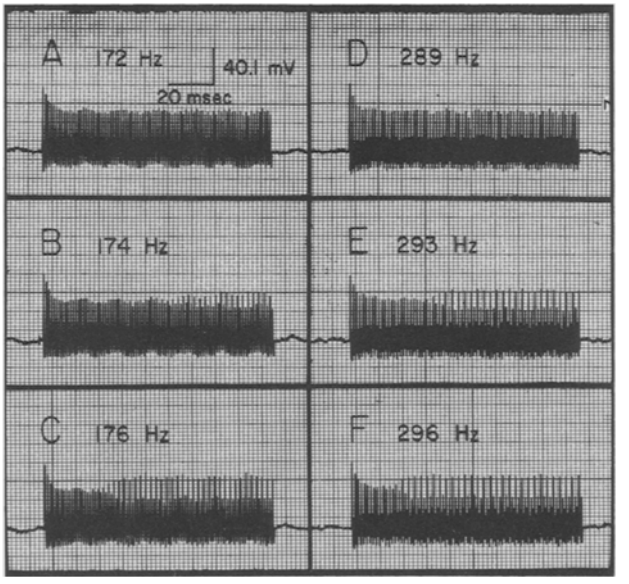

Fig. 6. Change in rotation number, R, with increasing frequency of stimulation. Axon responses to sinusoidal stimulation at 181 $\mu A/cm^2$ at various frequencies shown. (*A*): One response per sinusoidal stimulus ($R=1$). (*B*): A critical point appears at which R changes from 1 to 0.5. (*C*): Critical point occurs closer to onset of stimulation. (*D*): R equals 0.5. (*E*): A critical point appears at which R changes from 0.5 to 0.25. (*F*): Critical point occurs closer to onset of stimulation. Calibrations as noted. All measurements were taken on same axon at 10 °C.

response not by changing the amplitude of its response but by skipping spikes, with the spike size remaining nearly invariate. Figure 7*c* shows a steady-state periodic pattern which is slightly more complicated than some others, since it looks like a steady alternation of two simple patterns.

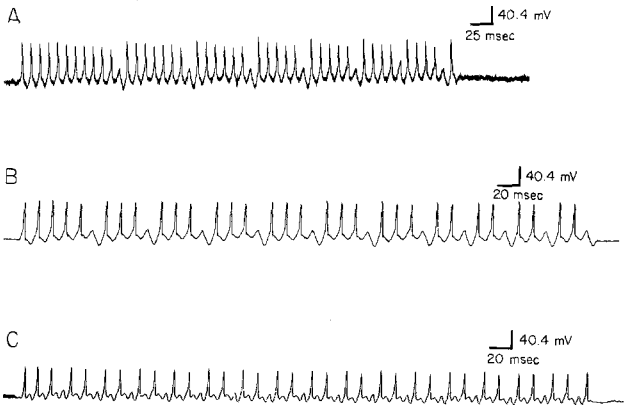

Fig. 7. In *A* and *B*, types of initial (nonsteady-state) responses of space-clamped squid axons to sinusoidal stimulation. (*A*): The pattern of firing is changing with time. The ratios of spikes to spikes plus misses decrease in small steps, *viz.*, 11:12(0.917), 7:8(0.875), 6:7(0.857), 5:6(0.833), and 4:5 (0.800). (*B*): Initial pattern, 3:4 changes with time to 2:3. (*C*): Ratios of 1:2 and of 1:3 alternate in the steadystate, giving a 2:5 ratio. (*A*): $f=100$ Hz; $I_{pp}=78.2$ $\mu A/cm^2$. (*B*): $f=80$ Hz; $I_{pp}=90.4$ $\mu A/cm^2$. (*C*): $f=160$ Hz; $I_{pp}=164.4$ $\mu A/cm^2$. 0 DC bias for *A*, *B*, and *C*.

Simulation Methods and Results

Simulations were done with CSMP-3 numerical analysis package available on the University of Illinois IBM 360/75 digital computer (Speckhart & Green, 1976). The Gear method for stiff differential equations was selected. Before settling on this numerical integration routine we did some computations on sinusoidal stimulation of the unmodified Hodgkin-Huxley model with various numerical integration methods, and compared our results with those of Holden (1976). In general we confirmed Holden's results, but there were some minor discrepancies. We found that the Runge-Kutta 4th order and Gear methods showed somewhat different positions of the boundaries between R-values than did the Euler method employed by Holden. We also found that the Gear method, which we believe was the most accurate, sometimes showed regular periodic values of R for stimulus parameters where other methods showed an apparently aperiodic response. Our interpretation of this finding is that sometimes a simulated R-value which is apparently irrational may be due not to inherent properties of the model but rather to errors in the numerical integration process. We are led to the belief that while most integration methods give generally similar results, the precise position in stimulus parameter phase space of the boundaries between R-values and the behavior of the model very near those boundaries is sensitive to the choice of integration method.

Our choice of numerical Hodgkin-Huxley parameters for the voltage-dependent channels and for the periaxonal space followed that of Adelman and Fitz-Hugh. For those parameters in the Jakobsson (1978*a*, *b*) model which have no counterpart in the H-H model, the multiplying factor K on k_{AA^*} was set equal to 20 for most simulations and the multiplying factor N on k_{AB} was set equal to 2 (Jakobsson, 1978*b*, Eq. (18)). These values of K and N were estimated in our previous work to give behavior typical of intact squid axons in normal seawater; i.e., very little inactivation shift, fairly large $\tau_c - \tau_h$ separation, and no repetitive firing in response to constant currents. For full equations describing the voltage-dependence of the channels, *see* the Appendix.

To simulate the noise, we imposed a sum of eighteen small sinusoidal currents to duplicate the power spectrum of current noise measured by Fishman et al. (1975). Their surface area was uncertain by a factor of 10 (10^{-4} to 10^{-5} m^2). We assumed a magnitude consistent with the area being the root mean square of the two extremes; i.e., 3.18×10^{-5} m^2. The measured noise varies with membrane potential. Since we expect the most important effects of the noise to be exerted near rest potential, when the axon is "deciding" to fire an action potential or not, we simulated the Fishman-Moore-Poussart measurements at rest. To simulate the effect of sucrose gap hyperpolarization, we set the reversal potential for the leakage conductance at -90 mV, on grounds that the rest potential is commonly hyperpolarized by about 30 mV in the sucrose gap. The amplitude of the leak conductance (g_L) was set empirically, after all the other model parameters were set, by adjusting it to give about the same threshold for giving action potentials in response to sinusoidal currents that we observed experimentally. In particular, we changed the g_L by increments of 0.1 mmho/cm^2 so that at 40 Hz and with a DC bias of 10.8 μA/cm^2, action potentials would just be elicited with a peak-to-peak intensity of about 40 μA/cm^2. The value of the g_L arrived at by this method was 0.9 mmho/cm^2, a bit larger than Adelman and FitzHugh's 0.7 mmho/cm^2 and much larger than the 0.3 mmho/cm^2 of the Hodgkin-Huxley model. We note that the threshold peak-to-peak stimulus intensity for producing action potentials is a very strong function of g_L; the threshold at 40 Hz was cut almost in half by a change from 0.9 to 0.8 mmhos/cm^2 and was raised by about the same amount by a change from 0.9 to 1.0 mmhos/cm^2.

The above procedures must be said to constitute estimates rather than determinations of the appropriate model parameters. Nevertheless it is reasonable to suppose that all of the ways in which we have modified the H-H formalism should make it a more realistic representation of our preparation. To determine all the numerical parameters in the fully modified model for our preparations would involve a separate study in itself, comprising several hundred clamp steps (to include all of the different aspects of Na^+ inactivation), several solution changes (to determine the effect of K^+ on Na^+ inactivation), and noise measurements. So we feel justified for now in estimating the parameters of the modified model in the hope that the simulations will provide at least some insight into why the system works the way it does. But we do emphasize a fundamental limitation in our analysis; i.e., we have not determined the numerical model parameters from the same population of axons on which we have done the sinusoidal current stimulation.

Table 2 shows the R-values exhibited by the computer model for a set of simulated experiments similar to those done on the real axon and shown in Table 1. The two tables are similar in some aspects of overall patterning of responses. For a particular frequency, R is a monotonically increasing function of stimulus intensity. As one increases frequency above 40 to 60 Hz at a given stimulus intensity, R is reduced. In both experiments and simulations, one sees occasionally an irrational value of R, corresponding to an apparently aperiodic response. In the simulations we can do something that we cannot do experimentally, namely shut off the noise. Therefore we redid without imposed noise all the computer runs in which an apparently irrational R was seen and found that in all cases but one elimination of the imposed noise made the membrane response become clearly periodic. In the simulations the imposed noise caused most of the apparent aperiodicity we observed. These results suggest to us that the apparent aperiodicity of some responses we saw experimentally could have been caused by channel conductance noise.

On the other hand, there are two major differences between the simulated results of Table 2 and the experimental results of Table 1: (i) at low frequency (20 Hz) and high amplitude of sinusoidal current modulation, our simulations gave responses with $R=2$, whereas the experiments never gave $R>1$, and (ii) our simulations almost never showed $R<0.5$, whereas $R<0.5$ was a very common experimental response for high frequencies and low sinusoidal current densities.

With respect to *i* above, the reason for the $R=2$ responses is that, contrary to our expectations, the computational model used to generate Table 2 was capable of giving more than one action potential when stimulated with a sustained current. Thus, for

Table 2. *R* as a function of frequency and intensity of stimulation for computer model of axon

Stimulus intensity[a] ($\mu A/cm^2$)	Frequency (Hz)									
	20	40	60	80	100	120	140	160	180	200
34.2	0									
37.8	0	0	0							
41.4	1	1	0	0						
45.0	1	1	1	0	0	0				
50.4				1	0.5	0				
54.0	1	1	1	1	0.844[b]	0	0			
57.6		1	1	1	1	0.5	0	0		
62.1	1				1	0.667	0.5	0	0	
70.2	1					1	0.5	0.5	0	
72.9						1	0.5	0.5	0.5	0
77.4							0.667	0.5	0.5	0.175[f]
82.8							0.8	0.5	0.5	0.5
86.4								0.5	0.5	
90							0.894[c]	0.5	0.5	
100									0.5	0.5
113.4	2					1	1	0.8	0.5	0.5
130									0.667	0.5
148.5	2						1	1	0.783[d]	0.5
180									1	0.691[e]
220.5									1	0.929($\frac{13}{14}$)
280									1	1
351									1	

[a] On a DC bias of 10.8 $\mu A/cm^2$. [b] 0.833 (5/6) w/o noise. [c] 898 w/o noise.
[d] 0.777 (7/9) w/o noise. [e] 0.692 (9/13) w/o noise. [f] 0.167 (1/6) w/o noise.

slow sinusoidal currents where the depolarizing phase lasted for a relatively long time, more than one action potential could be elicited during one phase of the stimulating current, giving $R=2$. After generating Table 2, we did some simulations in which we varied K (the multiplying factor on the rate constant from the resting to the excited state in the Na^+ channel kinetic model), using values of 15, 10, and 3.55. Both the multiple response of sustained current and $R>1$ in response to sinusoidal current were present for $K=15$ and 10 and not for $K=3.55$. We note that the unmodified Hodgkin-Huxley model yields $R>1$ for a wide range of stimulus parameters (Nemoto et al., 1975; Holden, 1976). These results confirm the intuitively reasonable connection between $R>1$ responses to sinusoidal current and repetitive responses to steady current but leave unanswered the question as to why the Adelman-FitzHugh (1975) modifications, which reduce the tendency of the H-H model to fire repetitively, apparently *increase* the tendency of the Jakobsson (1978*a*, *b*) model to fire repetitively (as measured by the values of the model parameter K at which repetitive firing is induced in response to suddenly applied sustained currents). At this writing, we do not know the answer to the latter question.

With respect to *ii* above, the relative rarity of computed R's less than 0.5, we can at least make a reasonable speculation. Noting that the "missing" responses would generally be of relatively long period (three or more times the period of the stimulus), we suspect that the absence of these responses is due to the existence of some very slow process not incorporated in our model. This suspicion is supported by simulations in which we attempted to reproduce the behavior of Figs. 6 and 7. In these results the system response changes quite gradually when a stimulus is applied which is very near a boundary between R-values. In computer simulations with our fully modified model, with the unmodified H-H model, and with the H-H model modified according to Adelman and FitzHugh, we did not see such gradual changes. Rather, we saw the system go almost immediately, within one or at most two response periods, to its steady-state value of R. We interpret this as further evidence that the experimental preparation's behavior may have been influenced by slow processes not incorporated in any of the models.

Sometimes the periodic responses of the noise-free computer model were quite complicated. For example, in Table 2 is shown for 180 $\mu A/cm^2$ and 200 Hz a noise-free response with $R=9/13$. This was made up of the following repeated pattern: 2 spikes—miss— 2 spikes—miss—2 spikes—miss—3 spikes—miss. Put another way, the system was oscillating regularly

between a 2/3 and 3/4 response, with three cycles at 2/3 and one at 3/4. When the noise was added, the system still oscillated between a 2/3 and 3/4 pattern, and each subpattern appeared with about the same frequency as in the noise-free system, but the oscillations became irregular; sometimes a 3/4 response would appear after two 2/3's, sometimes after three 2/3's, and sometimes after four 2/3's. The apparently irrational responses of the real axon were similarly made up of apparently stochastic fluctuations between simple subpatterns. Very rarely the real axon displayed *regular* oscillations between simple subpatterns; an example of such a response is shown in Fig. 7*c*. Such regular oscillations were also quite rare for the computer model with noise included. We never saw the exact pattern (2/5) of Fig. 7*c* on the computer model, but we did see an $R=3/5$ response (regular oscillations between $R=2/3$ and $R=1/2$) on the full computer model, including noise, for the following stimulus parameters: 174 Hz, 160 $\mu A/cm^2$ peak-to-peak, 0 DC bias.

From the above, we tend to believe that the apparently irrational R's seen in our experimental axons were caused by membrane noise. However, this cannot necessarily be generalized to all nerves in all cases, since the unmodified noise-free Hodgkin-Huxley axon gives apparently irrational R's for some stimulus parameters. This was reported by Holden (1976), and additional cases have been pointed out to us by Dr. John Rinzel (*personal communication*). We have verified some of these cases using the Gear method for solving stiff differential equations, so we believe that apparently irrational R's may be caused by other factors than noise in some systems. However, we believe that noise was the cause in our system.

Summary and Conclusions

Squid giant axons in a double sucrose gap apparatus were subjected to sinusoidally varying current stimuli, in which frequency, peak-to-peak current variation, and DC bias were varied. Characteristics of steady-state response and of the dynamics of achieving the steady state were observed. The experiments were simulated with a computer model which included effects of membrane noise, K^+ accumulation, Na^+ inactivation anomalies, and sucrose gap hyperpolarizing current, as well as the features of the conductance changes normally described by the Hodgkin-Huxley model. From our analysis we believe that all of the above effects, including noise, are significant determinants of the experimental system's response to periodic stimulation. In addition, we believe that some slow process or processes not included in our computer model probably affected the experimental axon's responses.

After submitting this paper for publication, we became aware of another study on sinusoidal current stimulation of squid axon (Fohlmeister, Adelman, Poppele, 1980, *Biophys. J. (in press)*). Their study used quite a different experimental protocol (high intensity sinusoid to drive the axon modulated by low intensity sinusoids of different frequency). Their results, like ours, suggest the existence of an asyet-uncharacterized slow process, since they see experimentally a low-frequency peak in their Bode plots which is not manifest in their computer simulations.

We have discussed this work with many and wish to acknowledge their help, especially Kenneth S. Cole, Bruce Knight, L.E. Moore, and John Rinzel.

This work was aided in part by NIH grant 5 R01 NS12272, awarded to R.G. Apparatus loaned by Harvey Fishman was purchased under his grant # NIH NS 11764. Computer time was provided by the Research Board of the University of Illinois. Final preparation of the manuscript was done while one of us (E. Jakobsson) was on sabbatical leave at the Department of Physiology, Duke University Medical Center, and we express appreciation for that Department's cooperation and use of their facilities.

Appendix

The full set of equations used in calculating Table 2 are as follows:

$$\dot{E}=[I-\bar{g}_{Na}B^3(E-E_{Na})-\bar{g}_K n^4(E-E_K) - \bar{g}_L(E-E_L)]/C \quad \text{(A1)}$$

where

I = applied current = DC bias + noise + amplitude $\times \sin(2\pi wt)$, $\mu A/cm^2$;
$\bar{g}_{Na}$ = maximum sodium conductance = 90 mmho/cm^2;
B = kinetic variable for sodium conductance, calculated as below;
E = transmembrane potential, mV;
E_{Na} = sodium reversal potential = 55 mV;
$\bar{g}_K$ = maximum potassium conductance = 42 mmho/cm^2;
n = Hodgkin-Huxley variable for potassium conductance, calculated as below;
E_K = potassium reversal potential, calculated as below;
$\bar{g}_L$ = leakage and sucrose gap conductance = 0.9 mmho/cm^2;
E_L = reversal potential for leakage and sucrose gap conductance = −90 mV;
C = membrane capacitance = 1 $\mu F/cm^2$.

The sodium kinetic variable B is calculated by the following set of equations:

$$\dot{A} = -(k_{AB} + k_{AC} + K\dot{f})\, A + k_{BA} B + k_{CA} C \tag{A2}$$

$$\dot{B} = k_{AB} A + k_{A^*B} A^* - (k_{BC} + k_{BA})\, B + k_{CB} C \tag{A3}$$

$$\dot{A}^* = K\dot{f} A - (k_{A^*B} + k_{A^*C})\, A^* \tag{A4}$$

$$C = 1 - A - B - A^* \tag{A5}$$

where the variables A, A^*, B, and C are the fractional populations of the activatable (resting), excited, conducting, and inactivated states, respectively (defined in Jakobsson, 1978*a*).

The coefficients in Eqs. (A2)-(A5) are voltage dependent and closely related to Hodgkin-Huxley rate constants (as modified by Adelman and Fitz-Hugh (1975)) as follows:

$$k_{A^*B} = \alpha_m = \frac{0.1(-35-E)}{\left[\exp\left(\frac{-35-E}{10}\right)-1\right]}\ \text{ms}^{-1} \tag{A6}$$

$$k_{BA} = \beta_m = 4\exp[(-60-E)/18]\ \text{ms}^{-1} \tag{A7}$$

$$k_{CA} = 2\alpha_h = 2[0.171385 - 0.0380856\ln(K_s)] \times \exp\left[\frac{-60-E}{27.4}\right]\text{ms}^{-1} \tag{A8}$$

$$k_{BC} = \frac{\beta_{h,E-10}}{3} = \frac{0.4534}{(1+\exp(-4-0.1111(E-10)))} + 0.004534\exp\left[\frac{-(E-10)K_s}{32.5K_s+185}\right]\text{ms}^{-1} \tag{A9}$$

$$k_{AB} = \beta_m m_\infty/(2-m_\infty)\ \text{ms}^{-1} \tag{A10}$$

where

$$m_\infty = \alpha_m/(\alpha_m+\beta_m)$$

$$f = m_\infty^6 - \exp\left(\frac{-(E+100)}{18}\right) \tag{A11}$$

$$K = \begin{matrix}20 \text{ when } \dot{V} \text{ is positive}\\ 0 \text{ when } \dot{V} \text{ is negative}\end{matrix} \tag{A12}$$

$$k_{A^*C} = k_{BC} \tag{A13}$$

$$k_{AC} = k_{CA}(1-h_\infty^{1/3})(1+k_{AB}/k_{BA})/h_\infty^{1/3} \tag{A14}$$

where

$$h_\infty = \alpha_h/(\alpha_h+\beta_h)$$

$$k_{CB} = k_{CA}k_{BC}k_{AB}/(k_{AC}k_{BA}) \tag{A15}$$

For the potassium kinetics:

$$\dot{n} = \alpha_n(1-n) - \beta_n n \tag{A16}$$

where

$$\alpha_n = \frac{0.005606(7.93-(E+60))}{\left[\exp\left(\frac{7.93-(E+60)}{7.93}\right)-1\right]}\ \text{ms}^{-1} \tag{A17}$$

$$\beta_n = 0.121866\exp\left[\frac{(-E-60)}{26.72}\right]\text{ms}^{-1} \tag{A18}$$

$$\dot{K}_s = (1/\theta)\,[10^{-6}(I_K/F) - 10^{-3}P_K^s(K_s-K_o)] \cdot \left(\frac{\text{mM}}{\text{liter}-\text{msec}}\right) \tag{A19}$$

where

θ = thickness of extracellular space = 3.79×10^{-6} cm;
I_k = potassium current, μA/cm^2;
F = Faraday's constant = 96,485 Coul/mole;
P_k^s = permeability of extracellular barrier = 3.4×10^{-4} cm/sec;
K_0 = bulk potassium concentration = 10 mmol/liter.

The factors 10^{-6} and 10^{-3} in the right hand terms of Eq. (A19) are to make the units of each of the equations terms commensurate with each other. The reversal potential for potassium is given by:

$$E_k = 24.172\ln\left(\frac{K_s}{K_i}\right)\text{mV} \tag{A20}$$

where $K_i = 248$ mmol/liter.

The noise was approximated, in μA/cm^2, by a sum of 18 sinusoidal terms:

$$\begin{aligned} I_{\text{noise}} = 3.16(&0.0303\cos(0.0942t)\\ &+0.0277\cos(0.1576)+0.0255\cos(0.22t)\\ &+0.0235\cos(0.283t)+0.0213\cos(0.345t)\\ &+0.019\cos(0.408t)+0.017\cos(0.471t)\\ &+0.0155\cos(0.534t)+0.014\cos(0.597t)\\ &+0.0346\cos(0.942t)+0.022\cos(1.57t)\\ &+0.018\cos(2.2t)+0.016\cos(2.83t)\\ &+0.0148\cos(3.45t)+0.0143\cos(4.08t)\\ &+0.041\cos(4.71t)+0.0139\cos(534t)\\ &+0.0137\cos(5.97t). \end{aligned} \tag{A21}$$

The magnitudes and frequencies in Eq. (A21) were selected to reproduce the power spectrum measured by Fishman et al. (1975). Essentially the measured power spectrum was divided into 18 segments, and

each segment was approximated by a single sinusoid. This method of simulating the noise was selected because trial computer runs with noise generated from random number generators caused enormously long computation times; our numerical integration routine had to make many attempts at each iteration to satisfy its error criteria, presumably since the "target" it was aiming at kept shifting.

References

Adelman, W.J., Jr., FitzHugh, R. 1975. Solutions of the Hodgkin-Huxley equations modified for potassium accumulation in a periaxonal space. *Fed. Proc.* **34**:1322

Adelman, W.J., Jr., Palti, Y. 1969. The influence of external potassium on the inactivation of sodium currents in the giant axon of the squid, *Loligo pealei*. *J. Gen. Physiol.* **53**:685

Fishman, H.M., Moore, L.E., Poussart, D.J.M. 1975. Potassium-ion conduction noise in squid axon membrane. *J. Membrane Biol.* **24**:305

Flaherty, J.B., Hoppenstaedt, F.C. 1978. Frequency entrainment of a forced van der Pol oscillator. *Stud. Appl. Math.* **58**:5

Guttman, R. 1969. Temperature dependence of oscillation in squid axons: Comparison of experiments with computations. *Biophys. J.* **9**:269

Hodgkin, A.L., Huxley, A.F. 1952. The dual effect of membrane potential on sodium conductance in the giant axon of *Loligo*. *J. Physiol. (London)* **116**:497

Holden, A.V. 1976. The response of excitable membrane models to a cyclic input. *Biol. Cybernetics* **21**:1

Jakobsson, E. 1978*a*. A fully coupled transient excited state model for the sodium channel. I. Conductance in the voltage clamped case. *J. Math. Biol.* **5**:121

Jakobsson, E. 1978*b*. A fully coupled transient excited state model for the sodium channel. II. Implications for action potential generation, threshold, respective firing, and accommodation. *J. Math. Biol.* **6**:235

Julian, F.J., Moore, J.W., Goldman, D.E. 1962. Membrane potentials of the lobster giant axon obtained by use of the sucrose-gap technique. *J. Gen. Physiol.* **45**:1195

Nemoto, I., Miyazaki, S., Saito, M., Utsunomiya, T. 1975. Behavior of solutions of the Hodgkin-Huxley equations and its relation to properties of mechanoreceptors. *Biophys. J.* **15**:469

Speckhart, F.H., Green, W.L. 1976. A Guide to Using CSMP—The Continuous System Modeling Program. Prentice-Hall, Englewood Cliffs

Received 12 November 1979